ON THE EXTREME POSITIVE STAR FORMATION FEEDBACK CONDITION IN SCUBA SOURCES

Sergiy Silich[1], Guillermo Tenorio-Tagle[1,4], Casiana Muñoz-Tuñón[2], Filiberto Hueyotl-Zahuantitla[1], Richard Wünsch[3], and Jan Palouš[3]

[1] Instituto Nacional de Astrofísica Optica y Electrónica, AP 51, 72000 Puebla, Mexico; silich@inaoep.mx
[2] Instituto de Astrofísica de Canarias, E 38200 La Laguna, Tenerife, Spain
[3] Astronomical Institute, Academy of Sciences of the Czech Republic, Boční II 1401, 141 31 Prague, Czech Republic

ABSTRACT

We present a detailed study of the hydrodynamics of the matter reinserted by massive stars via stellar winds and supernovae explosions in young assembling galaxies. We show that the interplay between the thermalization of the kinetic energy provided by massive stars, radiative cooling of the thermalized plasma, and the gravitational pull of the host galaxy lead to three different hydrodynamic regimes. These are: (1) the quasi-adiabatic supergalactic winds; (2) the bimodal flows, with mass accumulation in the central zones and gas expulsion from the outer zones of the assembling galaxy; and (3) the gravitationally bound regime, for which all of the gas returned by massive stars remains bound to the host galaxy and is likely to be reprocessed into further generations of stars. Which of the three possible solutions takes place depends on the mass of the star-forming region, its mechanical luminosity (or star formation rate), and its size. The model predicts that massive assembling galaxies with large star formation rates similar to those detected in Submillimeter Common-User Bolometric Array sources ($\sim$1000 $M_\odot$ yr^{-1}) are likely to evolve in a positive star formation feedback condition, either in the bimodal or in the gravitationally bound regime. This implies that star formation in these sources may have little impact on the intergalactic medium and result instead into a fast interstellar matter enrichment, as observed in high redshift quasars.

Key words: galaxies: formation – galaxies: high-redshift – galaxies: starburst – hydrodynamics

1. INTRODUCTION

In cosmology today the study of the star formation negative feedback is recognized as one of the central issues regarding galaxy formation (Dekel & Silk 1986; Friaca & Terlevich 1998; Tutukov et al. 2000; Scannapieco et al. 2002; Ferreras et al. 2002). The large UV photon output from massive stars and their violently deposited mechanical energy make them indeed major players in the dynamics of the interstellar matter (ISM) and key negative feedback agents able to limit and stop star formation defining the efficiency of the process (see Tenorio-Tagle & Bodenheimer 1988, Elmegreen 1999 and references therein). However, as shown by Tenorio-Tagle et al. (2005, 2007) and Wünsch et al. (2008) for the case of massive and compact super stellar clusters, this may not be the whole story as the stellar feedback may, in extreme cases, become positive. This would allow gravity to win over thermal pressure. This may also be the case if one considers star formation in the Submillimeter Common-User Bolometric Array (SCUBA) galaxies—high redshift sources with the highest ($\sim$1000 $M_\odot$ yr^{-1}) star formation rates (SFRs) known so far. These have been observed in the submillimeter continuum (emission from warm dust in the rest-frame far-IR/submillimeter wavelengths), in the CO line emission associated with the cold molecular gas, and in the near-infrared integral field spectroscopy, which deals with the rest-frame optical emission lines associated with the photoionized gas (see, for example, Hughes et al. 1998; Greve et al. 2005; Tacconi et al. 2006, 2008; Swinbank et al. 2006, and references therein).

The global properties of SCUBA galaxies include a typical dynamical mass of $5 \pm 3 \times 10^{11}$ $M_\odot$, a gas to dynamical mass fraction, $f_g = M_{\rm gas}/M_{\rm dyn} \sim 0.25$–$0.3$, and a ra-

dius of about 1–3 kpc, parameters consistent with the expected properties of massive spheroids in the early universe (Greve et al. 2005; Swinbank et al. 2006; Tacconi et al. 2006, 2008; Schinnerer et al. 2008). The long star formation duty cycle with a timescale $\sim$100–300 Myr and the inhomogeneous nature of SCUBA sources favor a continuous star formation scenario (Swinbank et al. 2006; Tacconi et al. 2008). Here we show how massive and violent star-forming events driven by a high rate of star formation lead to positive feedback. Looking at some extreme cases, we identify radiative cooling as the agent capable of downgrading the impact of the stellar energy deposition, leading inevitably to an extreme positive star formation feedback condition which should play a major role in galaxy formation. We also show that gravity is another major player. The gravitational pull of the galaxy also leads to a positive feedback condition, particularly in compact protogalactic sources. The gravitational pull then prevents the formation of a supergalactic wind, retaining the injected and ablated matter within the star-forming region, favoring its accumulation and conversion into future generations of stars.

In Section 2, we examine the physical implications of massive SFRs and discuss the physical limits between the various possible hydrodynamic regimes. The implications of events with a high SFR and our conclusions are given in Sections 3 and 4.

2. STAR FORMATION UNDER A LARGE SFR

If one scales the evolutionary synthesis models (e.g., Leitherer & Heckman 1995) for star clusters generated by a constant SFR to the values inferred from the SCUBA sources ($\geqslant$100 $M_\odot$ yr^{-1}; e.g., Greve et al. 2005; Swinbank et al. 2006; Tacconi et al. 2006), one sees that as a result of the continuous death and creation of massive stars, the UV photon output will level off at $\sim$10^{55} ionizing photons s^{-1} after 3 Myr of the evolution. The mechanical energy deposited by the evolving stars ($L_{\rm SF}$) through

---
[4] Sackler Visiting Fellow at the Institute of Astronomy, University of Cambridge, UK

winds and supernovae (SNe) will also increase, although not so rapidly, to reach a constant value $\sim 2.5 \times 10^{43}$ erg s^{-1} after 40 Myr of evolution. Accordingly, the mass violently returned to the ISM by stellar winds and supernovae will amount to $3 \times 10^7\, M_\odot$ after 10 Myr, reaching almost $10^9\, M_\odot$ after 100 Myr of evolution. The absolute values of all the above-mentioned variables ought to be linearly scaled by more than an order of magnitude, at the given times, if instead of a SFR equal to $100\, M_\odot$ yr^{-1}, one assumes the even larger values inferred for the most powerful SCUBA sources ($\geqslant 1000\, M_\odot$ yr^{-1}).

At first glance, such an energy deposition and such a vast amount of matter so violently injected would unavoidably lead to extreme massive outflows into the intergalactic medium (see, e.g., Heckman et al. 1990; Strickland & Stevens 2000; Scannapieco et al. 2002; Tenorio-Tagle et al. 2003; Veilleux et al. 2005, and references therein). Supergalactic winds are believed to result from the full thermalization of the kinetic energy of the ejecta through multiple random collisions within the star-forming volume (see Chevalier & Clegg 1985). Thermalization generates the large overpressure that continuously accelerates the deposited matter to finally blow it out of the star-forming volume, composing a stationary superwind with an adiabatic terminal speed $V_{A\infty} = (2L_{\rm SF}/\dot{M}_{\rm SF})^{1/2}$, where $L_{\rm SF}$ and $\dot{M}_{\rm SF}$ are the mechanical energy and mass deposition rates provided by stellar winds and supernovae explosions within the star-forming volume. For this to happen, the ejecta has to reach an outward velocity equal to the sound speed ($c = (\gamma P/\rho)^{1/2} \propto T^{1/2}$) right at the star-forming boundary, $R_{\rm SF}$, to then fulfill the stationary condition in which the rate at which matter is deposited equals the rate at which it streams away from the star-forming region: $\dot{M}_{\rm SF} = 4\pi R_{\rm SF}^2 \rho_{\rm SF} c_{\rm SF}$, where $\rho_{\rm SF}$ and $c_{\rm SF}$ are the values of density and sound speed at the surface of the star-forming region. However, as shown in the present series of papers (see Silich et al. 2003, 2004; Tenorio-Tagle et al. 2005, 2007; and Wünsch et al. 2008), when dealing with the outflows generated by massive bursts of star formation, the impact of radiative cooling becomes a relevant property, as is gravity, able to hold a fraction of the deposited matter within the star cluster volume.

In the case of an instantaneous burst of star formation, stellar winds and supernovae are able to remove the matter left over from star formation out of the star cluster volume in just a few megayears (Melioli & de Gouveia Dal Pino 2006; Tenorio-Tagle et al. 2006), and so the hydrodynamic solution considers only the matter reinserted by the massive stars. In the continuous star formation scenario, however, a gas reservoir out of which a constant SFR could be sustained is required. This implies that besides the mass returned by supernovae and stellar winds, $\dot{M}_{\rm SF}$, the flow may hold additional matter. This results from the destruction and mass ablation from star-forming clouds and can be normalized to the SFR within the star-forming region: $\dot{M}_{ld} = \eta_{ld}$SFR, where η_{ld} is the mass loading coefficient. The total mass input rate into the flow is then

$$\dot{M} = \dot{M}_{\rm SF} + \dot{M}_{ld} = \left(\frac{2L_0}{V_{A\infty}^2} + \eta_{ld} \times 1\, M_\odot\ {\rm yr}^{-1} \right) \frac{\rm SFR}{1\, M_\odot\ {\rm yr}^{-1}},$$
(1)

where L_0 is the normalization coefficient, which relates the mechanical energy output rate, $L_{\rm SF}$, to the SFR:

$$L_{\rm SF} = L_0({\rm SFR}/1\, M_\odot\ {\rm yr}^{-1}).$$
(2)

Hereafter we shall adopt $L_0 = 2.5 \times 10^{41}$ erg s^{-1} and $V_{A\infty} = 2750$ km s^{-1}. These values result from Starburst 99 synthetic models for a continuous star formation mode with

Table 1
Reference Models

Models	η_{ld}	Radii (kpc)	Dynamical Masses ($10^{11}\, M_\odot$)	SFRs ($M_\odot$ yr^{-1})	Regimes
(1)	(2)	(3)	(4)	(5)	(6)
1	0.5	2.5	2	2	Superwind
2	0.5	1.65	2	2	Superwind
3	0.5	1.2	2	2	Gravitationally bound
4	0.5	2.5	2	1200	Bimodal
5	0.5	1.7	2	1200	Bimodal
6	0.5	1.2	2	1200	Gravitationally bound

a Salpeter IMF and sources between $0.1\, M_\odot$ and $100\, M_\odot$, for ages $t \geqslant 40$ Myr (Leitherer et al. 1999). Note that mass loading changes the outflow terminal speed, which in this case is smaller than $V_{A\infty}$:

$$V_\infty = \left(\frac{2L_{\rm SF}}{\dot{M}_{\rm SF} + \dot{M}_{ld}} \right)^{1/2} = \frac{V_{A\infty}}{\left(1 + \frac{1\, M_\odot\ {\rm yr}^{-1} \eta_{ld} V_{A\infty}^2}{2L_0} \right)^{1/2}}.$$
(3)

For the calculations, our semi-analytic radiative stationary wind code (Silich et al. 2008) and the one-dimensional hydrocode ZEUS3D (Stone & Norman 1992) as modified by Tenorio-Tagle et al. (2007) and Wünsch et al. (2008) were used. All numerical calculations were performed with open inner and outer boundary conditions. The hydrodynamic equations here include the gravitational pull from the baryonic and dark matter, both assumed to be homogeneously distributed inside the star-forming region. In our approach, it is also assumed that the mass of the flow is negligible compared to the dynamical mass of the system, and thus the self-gravity of the reinserted gas is not included in the calculations. For example, the mass of the flow within the star-forming region, $M_{\rm flow}$, normalized to the dynamical mass of the system is $M_{\rm flow}/M_{\rm dyn} \approx 2 \times 10^{-5}$ and $M_{\rm flow}/M_{\rm dyn} \approx 8 \times 10^{-3}$ in the case of model 1 with a low SFR and model 4 with a high SFR, respectively. To obtain the stationary hydrodynamic solution one has to know the mechanical energy and mass deposition rates, which are defined by Equations (1) and (2), and the radius of the star-forming region, $R_{\rm SF}$. We use the equilibrium cooling function, $\Lambda(T, Z)$, tabulated by Plewa (1995) and set the metallicity of the plasma to the solar value in all calculations. Our reference models are presented in Table 1. Here Column 1 marks the model in our list, the ablation coefficient, η_{ld}, is presented in Column 2, Columns 3, 4, and 5 present the radius, dynamical mass of the star-forming region, and the SFR, respectively. Column 6 provides information regarding the resultant hydrodynamic regime.

3. THE HYDRODYNAMIC REGIMES

There are three major hydrodynamic regimes that develop within galaxies undergoing a large SFR. Which of the three possible solutions takes place depends on the mass of the star-forming region and its position in the mechanical luminosity or SFR versus size ($R_{\rm SF}$) parameter space. Figure 1 presents the threshold lines, which separate protogalaxies evolving in different hydrodynamic regimes. The left panel presents threshold lines for protogalaxies whose dynamical mass is equal to $2 \times 10^{11}\, M_\odot$ for different values of the ablation coefficient ($\eta_{ld} = 0.1, 05, 1.0$, dotted, solid, and dashed lines, respectively). Below the threshold lines, radiative cooling has a negligible effect on the flow and the reinserted matter ends up as
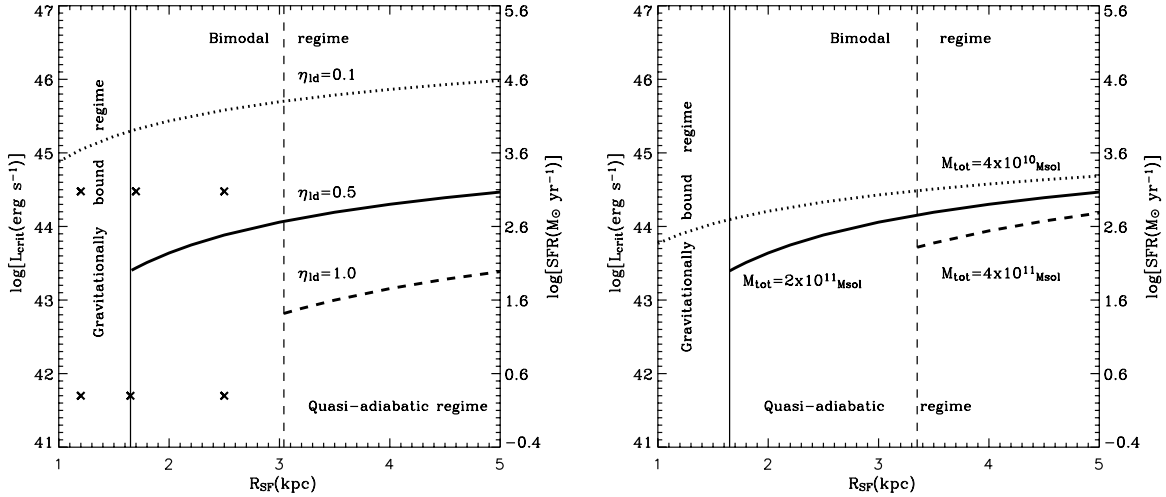
Figure 1. Threshold SFR or energy input rate vs. the threshold size. The left panel displays the threshold mechanical luminosity, SFR, and critical radii for different values of η_{ld} in the case when the dynamical mass in the star-forming system $M_{dyn} = 2 \times 10^{11}\ M_\odot$. The limiting energy input rate and its corresponding constant SFR (right-hand axis) above which strong radiative cooling inhibits the stationary superwind solution, as a function of the size of the star-forming region and the mass ablation coefficient, η_{ld}. These are terminated at the vertical lines, which display the critical radii, R_{crit}. Gravity inhibits the formation of supergalactic winds in systems with smaller radii. The right-hand panel shows how the location of the threshold lines depends on the total mass of the star-forming region. Several of the cases here presented are marked by crosses in the left panel. Note that the vertical line that marks the critical radius (R_{crit}) for $\eta_{ld} = 0.1$ in the left panel, and for $M_{dyn} = 4 \times 10^{10}\ M_\odot$, in the right panel, lies within 1 kpc and thus is not shown.

a superwind. Above these lines, radiative cooling leads to a bi-modal regime in which some of the reinserted matter within the densest central regions loses its pressure and is unable to participate in the galactic wind. Instead, it accumulates there, fueling further stellar generations (Tenorio-Tagle et al. 2005; Wünsch et al. 2008). For compact star-forming regions, to the left of the vertical lines shown in Figure 1 ($R_{SF} < R_{crit}$), gravity inhibits the formation of a superwind, leading instead to matter accumulation and to further generations of star formation. In these cases, the sound speed at the surface of the star-forming region is smaller than $\sim (GM_{dyn}/2R_{SF})^{1/2}$, which is one half of the escape speed from the protogalaxy surface. The threshold lines for less ($4 \times 10^{10}\ M_\odot$) and more ($4 \times 10^{11}\ M_\odot$) massive galaxies with $\eta_{ld} = 0.5$ are presented in Figure 1, right-hand panel.

As initially expected (see Section 2), there is a large fraction of the parameter space that leads to stationary supersonic winds. In these cases, all the deposited matter, as well as that ablated from clouds, is able to escape from the gravitational well of the galaxy. For this to happen, the flow has its stagnation point (the point where the velocity of the flow equals 0 km s^{-1}) right at the center of the galaxy ($R_{st} = 0$ pc) and its sonic point at the surface. The matter accelerates then through pressure gradients to reach supersonic velocities and form a supergalactic wind as it streams away from the galaxy.

Models 1 and 2 in Table 1 undergo such supergalactic winds. The distribution of the hydrodynamical variables in this case is shown in Figure 2. Here panel (a) presents the flow velocity (solid line) in the case of model 1 and compares this to the local sound speed, $(\gamma P(r)/\rho(r))^{1/2}$ and $V_{esc}(r) = (2GM(r)/r)^{1/2}$, which is the escape velocity at any distance r outside the star-forming region. The outflow velocity reaches the local sound speed value right at the surface of the star-forming region, then it accelerates rapidly to reach its terminal value of ~ 740 km s^{-1} at a distance about 4 kpc from the galaxy center. At this distance, it already exceeds the escape velocity and thus composes a supergalactic wind. Panels (b) and (c) present the distributions of temperature and density in the flow. The temperature drops from $\sim 2 \times 10^7$ K inside of the star-forming region to $\sim 2 \times 10^6$ K

at a 10 kpc distance from the galaxy, whereas the density drops from $\sim 4 \times 10^{-3}$ cm^{-3} to less than 10^{-4} cm^{-3} value. Such protogalactic winds should be detected as sources of a diffuse X-ray emission, as is the case in the local universe (e.g., Chevalier 1992; Strickland & Stevens 2000; Silich et al. 2005; Strickland & Heckman 2009):

$$L_X = 4\pi \int_{R_{st}}^{R_{out}} r^2 n^2 \Lambda_X(T, Z)dr, \qquad (4)$$

where $n(r)$ is the atomic number density, $\Lambda_X(Z, T)$ is the X-ray emissivity (see Strickland & Stevens 2000), and R_{out} marks the distance at which the calculations where stopped, usually set to 10 kpc. We set the lower integral limit to R_{st} assuming that the X-ray emission interior to it is completely absorbed by the accumulated gas. The model predicts a growth in the X-ray luminosity in the range from 0.3 to 8.0 keV as one considers larger SFRs. It is $L_x \approx 4 \times 10^{-4} L_{SF} \approx 2 \times 10^{38}$ erg s^{-1} and reaches $L_x \approx 0.1 L_{SF} \approx 3 \times 10^{43}$ erg s^{-1} (compare to Laird et al. 2010) in the case of model 1 with a low SFR and model 4 with a high SFR, respectively. Note that the X-ray emission is concentrated toward the star-forming region, where the density of the X-ray plasma reaches its maximum value and that in protogalaxies with a high SFR a significant fraction of this emission may be absorbed by numerous dense protostellar clouds.

However, in the case of SCUBA sources gravity may affect the outflow significantly. Indeed, the escape speed at the surface of scuba sources, $V_{esc} = (2GM_{dyn}/R_{SF})^{1/2}$, may reach ~ 1000 km s^{-1}, value which is approximately 10 times larger than in the case of young stellar clusters. In many cases, it is larger than the sound speed in the thermalized plasma, and thus larger than the outflow velocity at the surface of the protogalactic cloud. The larger impact of gravity on the flow for progressively more compact systems with the same mass is shown in Figure 2(d), which compares the run of velocity for models 1 and 2 (solid and dashed lines, respectively). The maximum velocity is much smaller, and the flow velocity drops significantly with distance to the protogalactic cloud in the case
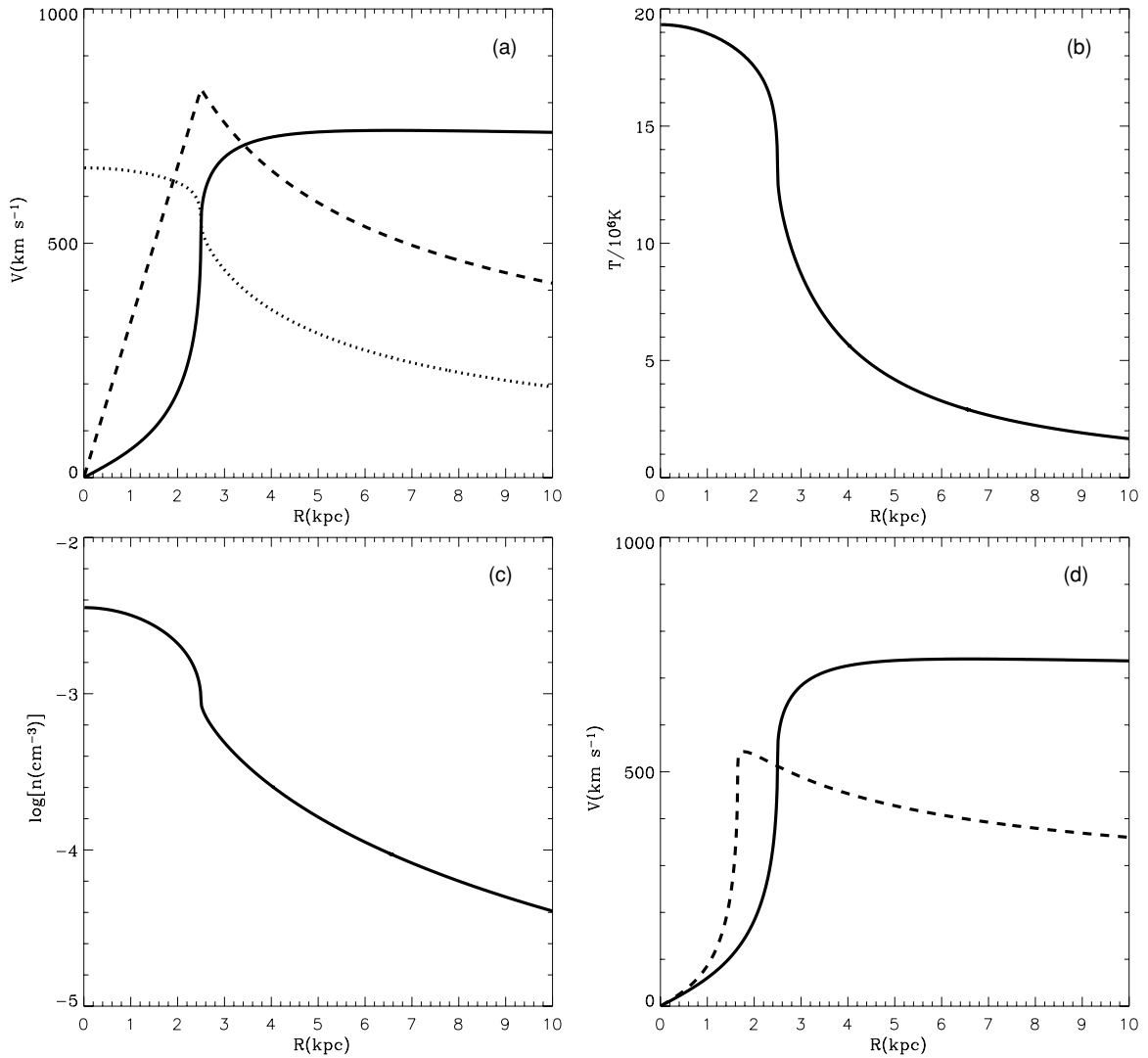
Figure 2. Distribution of hydrodynamical variables in the supergalactic wind outflow. The calculations were provided for a protogalaxy with a dynamical mass of $M_{\rm dyn} = 2 \times 10^{11}\ M_\odot$, $R_{\rm SF} = 2.5$ kpc, SFR $= 2\ M_\odot$ yr^{-1}, and $\eta_{ld} = 0.5$ (model 1). Panels (a), (b), and (c) present the run of velocity, temperature, and particle number density, respectively. The dotted and dashed line in panel (a) display the local sound speed and the value of $V_{\rm esc}(r)$, respectively. Panel (d) compares the velocity distribution in two protogalactic winds emerging from sources of different size (models 1 and 2, solid and dashed lines, respectively).

of more compact star-forming region (model 2, dashed line). Nevertheless, it ends up exceeding the escape velocity value at a larger distance from the protogalaxy center, forming a supergalactic wind.

Protogalaxies which lie above the threshold line (models 4 and 5) radiate a large fraction of the energy input rate within the star-forming volume, which leads to a bimodal hydrodynamic solution (Tenorio-Tagle et al. 2007; Wünsch et al. 2008). In this case, radiative cooling rapidly depletes the thermal energy (and pressure) of the thermalized plasma in the densest central regions of the assembled galaxy, inhibiting the fast acceleration required to reach the sufficient speed to leave the star-forming region. This prompts the stagnation radius, $R_{\rm st}$, to move out of the starburst center as is shown in Figure 3, left panel, where the solid and dotted lines display the semi-analytic results for models 4 and 5, respectively. Inside the stagnation radius, the stationary solution does not exist and thus one cannot apply the semi-analytic model to this region (Tenorio-Tagle et al. 2007; Wünsch et al. 2008). However, in Figure 3, right panel, we show the semi-analytic velocity distribution (solid line) in the case of model 4 and compare this with the full numerical simulations

(open circles) carried out with our Eulerian hydrodynamic code. The code also includes the gravitational pull from the matter located inside the star-forming region and a modified cooling routine, which allows for extremely fast cooling regimes (Tenorio-Tagle et al. 2007; Wünsch et al. 2008). The numerical simulations show an excellent agreement with our semi-analytic results. Both the positions of the stagnation point and the velocity profiles outside of the stagnation radius obtained with the semi-analytic and one-dimensional simulations are in good agreement. Thus, above the threshold line the matter injected by massive stars and ablated from protostellar clouds inside the stagnation volume remains bound and is reprocessed into new generations of stars despite the large amount of energy supplied by stellar winds and supernovae explosions. At the same time, the matter deposited by massive stars outside of this volume flows away from the star-forming region as a supersonic wind.

The impact of gravity becomes a crucial issue if the radius of the protogalaxy is smaller or equal to the critical value, presented in Figure 1 by vertical lines for different values of η_{ld} and $M_{\rm dyn}$. This occurs when the sound speed at the surface of the protogalactic cloud becomes smaller than one half of the
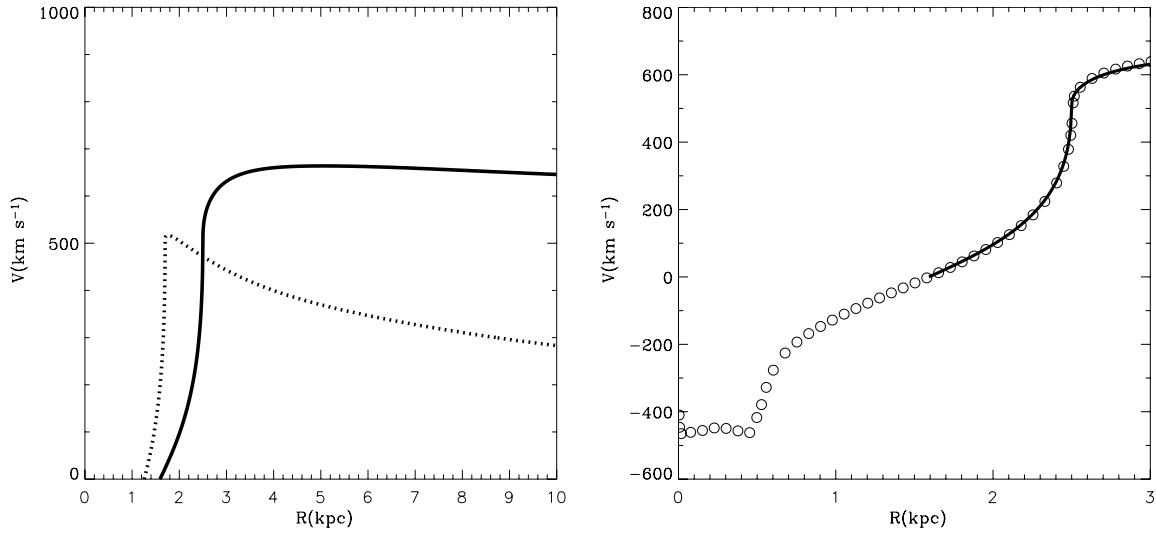
Figure 3. Velocity of the flow for protogalactic sources evolving in the bimodal hydrodynamic regime. The calculations were carried out for a protogalactic cloud with a dynamical mass of $M_{dyn} = 2 \times 10^{11}\,M_\odot$, SFR = 1200 $M_\odot$ yr^{-1}, and $\eta_{ld} = 0.5$. The left panel presents the results of the semi-analytic calculations for protogalaxies with $R_{SF} = 2.5$ kpc and $R_{SF} = 1.7$ kpc—solid and dotted lines, respectively. In the right panel, the semi-analytic velocity distribution for model 4 (solid line) is compared with the numerical results (open circles).
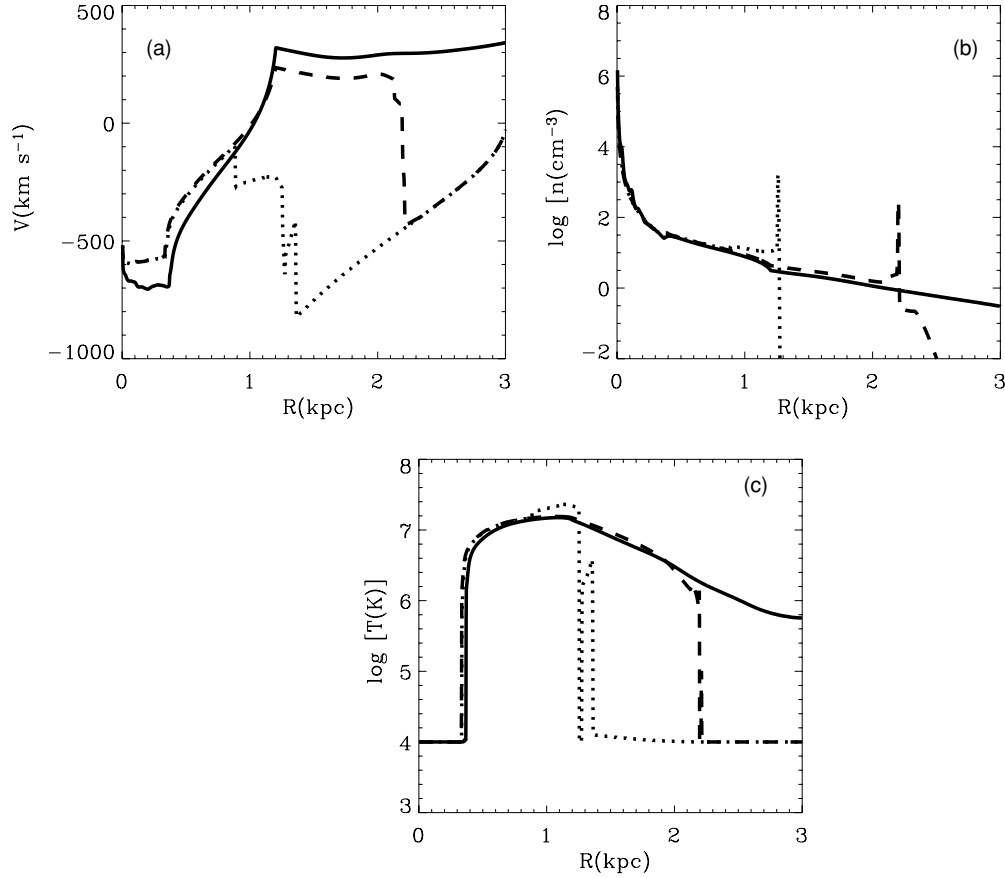
Figure 4. Gravitationally bound regime. Panels (a), (b), and (c) present runs of velocity, density, and temperature at t = 22.2 Myr, 29.5 Myr, and 31.4 Myr (solid, dashed, and dotted lines, respectively) in case 6 from Table 1.

escape velocity, and the nominator in the momentum equation (Equation (12) in Silich et al. 2008) goes to zero at the surface of the star-forming region. In this case, the flow velocity cannot exceed the sound speed value, the stationary solution vanishes, and the protogalaxy does not form a supergalactic wind. This regime is illustrated in Figure 4, which presents the results of full numerical simulations for a protogalactic cloud with

$R_{SF} < R_{crit}$ (model 6). Here the quasi-adiabatic wind solution for a protogalaxy with $M_{dyn} = 2 \times 10^{11}\,M_\odot$, $R_{SF} = 2.5$ kpc, SFR = 40 $M_\odot$ yr^{-1}, and $\eta_{ld} = 0.5$ was used as the initial condition for simulations. However, the time evolution was followed assuming the input parameters of model 6 (see Table 1). The initial wind solution transforms rapidly into a complex flow with a number of discontinuities and negative velocities inside
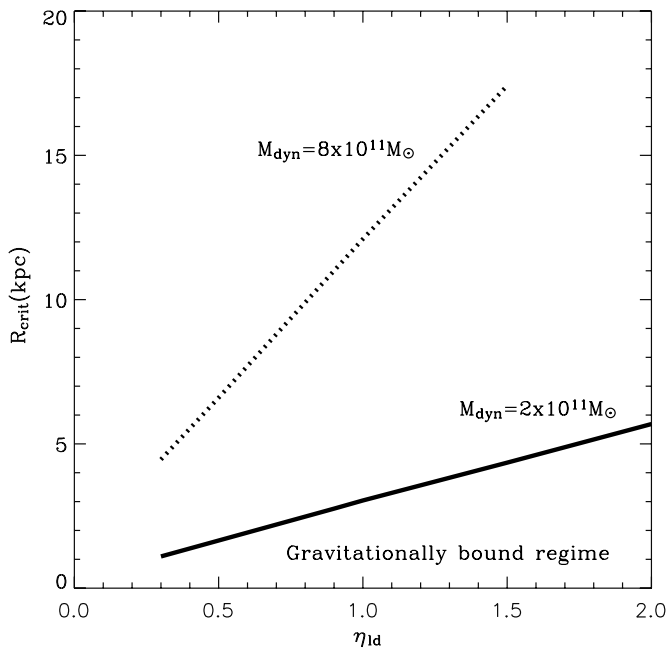
Figure 5. Critical size ($R_{\rm crit}$) of star-forming regions as a function of the ablation parameter η_{ld} and the dynamical mass of the protogalaxy. The superwind feedback mode is inhibited in protogalaxies with $R_{\rm SF} < R_{\rm crit}$. The matter returned by massive stars and ablated from star-forming regions remains buried inside the star-forming volume and as it accumulates it should lead to further stellar generations. The calculations were provided for protogalactic clouds with $0.3 \leqslant \eta_{ld} \leqslant 2$ and dynamical masses of $M_{\rm dyn} = 2 \times 10^{11}\ M_\odot$ (solid) and $M_{\rm dyn} = 8 \times 10^{11}\ M_\odot$ (dotted) lines, respectively.

the star-forming region. Note that the stagnation radius is in this case at $\sim$1 kpc. However, the matter deposited between this radius and the edge of the star-forming region is unable to produce a superwind and instead it cools down and ends up falling toward the center. Our open boundary condition does not allow for the accumulation of this gas and that leads after a readjustment period to a recurrent cycle in which some fraction of the deposited matter first flows away but then cools down and falls back toward of the star-forming region. This causes the compression and storage of the hot gas into a dense shell, which is driven inwards by gravity. The supersonic encounter of the outer gas with the dense shell results into the formation of a shock wave. This at later times ($t > 30$ Myr; dotted lines in Figure 4) produces the parcel of hot gas infalling behind the cold shell. The shell drives at all times a sound wave into the hot inner zones, which results into noticeable enhancement of temperature and speeds up the infalling gas ahead of the shell as it is displayed by the dotted line in Figure 4. The simulation ended up at $\sim$30 Myr when all matter located inside a computational domain is falling toward the center of the protogalactic cloud.

Thus, compact protogalaxies with $R_{\rm SF} < R_{\rm crit}$ trap the injected matter and are not able to form superwinds regardless of their energy output or SFR. A number of semi-analytic calculations have led us to infer that below the mechanical luminosity threshold line, $R_{\rm crit}$ becomes slightly smaller for protogalaxies with a given $M_{\rm dyn}$, and η_{ld} and a decreasing SFR. However, the calculations showed that the difference in the value of the critical radius usually does not exceed $\sim$100 pc. Therefore, we have adopted the value of $R_{\rm crit}$, calculated for a protogalaxy with the threshold SFR as the gravitationally bound limit for all galaxies with the same $M_{\rm dyn}$ and η_{ld}. The adopted critical radii, $R_{\rm crit}$, for galaxies with various $M_{\rm dyn}$ and η_{ld} are

displayed in Figure 1 by thin vertical lines. Figure 5 shows how the critical radius depends on η_{ld} and the dynamical mass of the system.

Note that in very high redshift systems (i.e., just forming galaxies) the metallicity would be extremely low and hence radiative cooling will be substantially lowered. This could potentially have a large effect on the dynamics of the reinserted matter, favoring outflows. While this may be true for the first galaxies, observationally it is known that the metallicity of high redshift systems can be large in some cases, reaching values of several times solar. If metallicity grows rapidly as the galaxy forms, then radiative cooling will be even stronger than that predicted in our calculations further favoring the retention of the reinserted material. The threshold SFR line in Figure 1 moves up a factor of 1.5 approximately in the case of the first galaxies with a metallicity $Z = 0.1\ Z_\odot$ and approximately 4.5 times down for older systems with a super-solar abundance ($Z = 10\ Z_\odot$). Note that the critical radii, $R_{\rm crit}$, remain almost identical as one considers different metallicities. A time-dependent solution accounting for the rapid change in the metallicity of the reinserted matter will be the subject of a forthcoming communication.

4. DISCUSSION

We have shown here that the thermalization of the kinetic energy provided by vigorous star formation in young forming galaxies may lead to three different hydrodynamic regimes, depending on the rate of star formation, the protogalaxy total mass and radius, and the rate of mass loading from protostellar clouds. Large galaxies with low SFRs and small ablation coefficient η_{ld} form supersonic winds which carry from the star formation regions the matter returned by massive stars and that ablated from protostellar clouds. Similar galaxies located in the SFR–$R_{\rm SF}$ parameter space above the threshold line lose via a superwind a fraction of the deposited matter. The matter deposited by massive stars and that ablated from star-forming regions in the inner zones of such galaxies becomes thermally unstable due to strong radiative cooling, accumulates and is to be re-processed there into secondary star formation. Finally, the thermal pressure in compact sources with radii $R_{\rm SF} \leqslant R_{\rm crit}$ is unable to withstand the gravitational pull of the galaxy. In such cases, protogalaxies retain all the reinserted and ablated matter within the protogalaxy volume and do not form supergalactic winds.

The value of the ablation parameter η_{ld} remains free in the theory. However, one can get an idea about which values of η_{ld} are reasonable considering sources without a secondary star formation, which evolve in the superwind regime. Then one can notice that in the case of star formation with a constant SFR, which terminates when the initial gas reservoir is completely exhausted, the global star formation efficiency, ϵ_*, defined as the ratio of the stellar mass, M_*, to the initial mass, $M_{\rm PG}$, of the protogalactic cloud at this moment will be

$$\epsilon_* = \left({\rm SFR} - \frac{2L_0}{V_{A\infty}^2} \frac{\rm SFR}{1\ M_\odot\ {\rm yr}^{-1}} \right) ({\rm SFR} + \eta_{ld} {\rm SFR})^{-1} = \frac{0.9}{1 + \eta_{ld}}.$$
(5)

In Equation (5), the stellar mass, M_*, was calculated as the difference between the mass of stars formed during the evolutionary time t and that reinserted by supernovae explosions and

stellar winds:

$$M_* = (\text{SFR} - \dot{M}_{\text{SF}}) \times t = \left(\text{SFR} - \frac{2L_0}{V_{A\infty}^2} \frac{\text{SFR}}{1\,M_\odot\,\text{yr}^{-1}} \right) \times t, \quad (6)$$

and the initial mass of the system, M_{PG}, is

$$M_{\text{PG}} = (1 + \eta_{ld}) \times \text{SFR} \times t. \quad (7)$$

The star formation efficiency would then be $\epsilon_* = 90\%$ if $\eta_{ld} = 0$ and approaches $\approx 30\%$ value required to form a gravitationally bound system (e.g., Geyer & Burkert 2001) when $\eta_{ld} = 2$. Note that the required star formation efficiency may be smaller, and thus the upper limit for η_{ld} larger, if one considers a slow expulsion of the injected gas from the system (Baumgardt & Kroupa 2007).

The predictions are thus that massive star-forming proto-galaxies with large SFRs similar to those detected in SCUBA sources ($\geqslant 10^3\,M_\odot\,\text{yr}^{-1}$) evolve in a positive star formation feedback conditions: either in the bimodal, or in the gravitationally bound regime. Only protogalaxies evolving in the bimodal regime will form supergalactic winds as is in the case of sub-millimeter galaxies SMM J14011+0252 (Nesvadba et al. 2007) and, probably, SMM J221726+0013 (Bower et al. 2004). In-evitably then, matter accumulation would follow in the central zones or in the whole protogalactic volume. Radiative cooling would then reduce the injected gas temperature, which would promote an even stronger cooling and recombination, making the accumulated gas an easy target of the UV radiation field. Photoionization of this gas is to set an equilibrium temperature ($T_{\text{H\,II}} \leqslant 10^4$ K), causing it to become Jeans unstable, leading un-avoidably to its collapse and to the formation of new stars. Many stellar generations are expected in this scenario, until most of the mass, through its continuous recycling, has been converted into low mass stars with $M \leqslant 7\,M_\odot$. The resultant stellar populations and the ISM would then show a large metallicity spread.

Consequently, if the formation of large stellar spheroids (galaxy bulges or elliptical galaxies) occurs through a process of rapid matter accumulation and further conversion of this matter into stars (e.g., Swinbank et al. 2006), which would imply a large SFR, the expectations are thus that little or none of the returned matter, through winds and SN explosions, is going to be ejected out of the system. Instead it is to be reprocessed into further episodes of stellar formation. This implies that the largest episodes of star formation would leave little trace of their stellar evolution into the intergalactic medium leading instead to a fast metal enrichment of the interstellar gas, as observed in high redshift quasars (e.g., Hamann & Ferland 1999; Juarez et al. 2009). The hydrodynamics of star-bursting galaxies with a central supermassive black hole will be the subject of a further communication.

REFERENCES

Baumgardt, H., & Kroupa, P. 2007, MNRAS, 380, 1589
Bower, R. G., et al. 2004, MNRAS, 351, 63
Chevalier, R. A. 1992, ApJ, 397, L39
Chevalier, R. A., & Clegg, A.W. 1985, Nature, 317, 44
Dekel, A., & Silk, J. 1986, ApJ, 303, 39
Elmegreen, B. G. 1999, ApJ, 517, 103
Ferreras, I., Scannapieco, E., & Silk, J. 2002, ApJ, 579, 247
Friaca, A. C. S., & Terlevich, R. J. 1998, MNRAS, 298, 399
Geyer, M. P., & Burkert, A. 2001, MNRAS, 323, 988
Greve, T. R., et al. 2005, MNRAS, 359, 1165
Hamann, F., & Ferland, G. 1999, ARA&A, 37, 487
Heckman, T. M., Armus, L., & Miley, G. K. 1990, ApJS, 74, 833
Hughes, D. H., et al. 1998, Nature, 394, 241
Juarez, Y., et al. 2009, A&A, 494, L25
Laird, E. S., Nandra, K., Pope, A., & Scott, D. 2010, MNRAS, 401, 2763
Leitherer, C., & Heckman, T.M. 1995, ApJS, 96, 9
Leitherer, C., et al. 1999, ApJS, 123, 3
Melioli, C., & de Gouveia Dal Pino, 2006, A&A, 445, L23
Nesvadba, N. P. H., et al. 2007, ApJ, 657, 725
Plewa, T. 1995, MNRAS, 275, 143
Scannapieco, E., Ferrara, A., & Madau, P. 2002, ApJ, 574, 590
Schinnerer, E., et al. 2008, ApJ, 689, L5
Silich, S., Tenorio-Tagle, G., & Añorve Zeferino, G.A. 2005, ApJ, 635, 1116
Silich, S., Tenorio-Tagle, G., & Hueyotl-Zahuantitla, F. 2008, ApJ, 686, 172
Silich, S., Tenorio-Tagle, G., & Muñoz-Tuñón, C. 2003, ApJ, 590, 796
Silich, S., Tenorio-Tagle, G., & Rodríguez González, A. 2004, ApJ, 610, 226
Stone, J. M., & Norman, M. L. 1992, ApJS, 80, 753
Strickland, D. K., & Heckman, T. M. 2009, ApJ, 697, 2030
Strickland, D. K., & Stevens, I. R. 2000, MNRAS, 314, 511
Swinbank, A. M., Chapman, S. C., Smail, I., Lindner, C., Borys, C., Blain, A. W., Ivison, R. J., & Lewis, G. F. 2006, MNRAS, 371, 465
Tacconi, L. J., et al. 2006, ApJ, 640, 228
Tacconi, L. J., et al. 2008, ApJ, 680, 246
Tenorio-Tagle, G., & Bodenheimer, P. 1988, ARA&A, 26, 145
Tenorio-Tagle, G., Muñoz-Tuñón, C., Pérez, E., Silich, S., & Telles, E. 2006, ApJ, 643, 186
Tenorio-Tagle, G., Silich, S., & Muñoz-Tuñón, C. 2003, ApJ, 597, 279
Tenorio-Tagle, G., Silich, S., Rodríguez-González, A., & Muñoz-Tuñón, C. 2005, ApJ, 628, L13
Tenorio-Tagle, G., Wünsch, R., Silich, S., & Palouš, J. 2007, ApJ, 658, 1196
Tutukov, A. V., Shustov, B. M., & Wiebe, D. S. 2000, Astron. Rep., 44, 711
Veilleux, S., Cecil, G., & Bland-Hawthorn, J. 2005, ARA&A, 43, 769
Wünsch, R., Tenorio-Tagle, G., Palouš, J., & Silich, S. 2008, ApJ, 683, 683